ISSN: 2096-3246

Volume 54, Issue 06, Nov 2022

TEMPERATURE-SENSITIVITY OF TWO MICROWAVE HEMT DEVICES: ALGAAS/GAAS VS. ALGAN/GAN HETEROSTRUCTURES

[1]*P. IMRAN KHAN,*[2] *Dr.J.KALIAPPAN*

Department Of ECE

St. Johns College of Engineering & Technology, Errakota, Yemmiganur

Keywords:
Gallium Arsenide (GaAs); Gallium Nitride (GaN); heterostructure; high electron-mobility transistor (HEMT); microwave performance; temperature-sensitivity

ABSTRACT

This research aims to conduct a comparative investigation of the heat effects on the microwave performance of high electron-mobility transistors (HEMTs) using GaAs and GaN technology. In order to achieve this difficult objective, the impact of changes in the surrounding temperature on the microwave performance is assessed by using scattering parameter data and the related equivalent-circuit models. The devices under investigation are two High Electron Mobility Transistors (HEMTs) with an identical gate width of 200 µm. However, they are manufactured utilizing distinct semiconductor materials: GaAs and GaN technologies. The examination is conducted under controlled settings of both low and high temperatures, with the temperature range being adjusted from -40 ◦C to 150 ◦C. The temperature's influence varies significantly based on the chosen operating state. However, the bias point is picked to provide a fair comparison between the two distinct technologies to the greatest extent feasible. Both technologies exhibit similar tendencies, although the temperature has a greater influence on the GaN device.

ISSN: 2096-3246
Volume 54, Issue 06, Nov 2022

I. INTRODUCTION

High electron-mobility transistors (HEMTs, also known as a heterostructure or heterojunction FETs) based on AlGaAs/GaAs and AlGaN/GaN heterostructures have greatly evolved since their inception in the early 1980s [1] and early 1990s [2], respectively. The most evident difference between the GaAs and GaN technologies is that the former is more mature, whereas the latter is more suited for high-power applications, owing to its wide bandgap nature. Over the years, many studies have focused on the high-frequency characterization and modeling of the temperature-dependent behavior of both GaAs [3–12] and GaN [13–27] HEMTs. This is because the operating temperature can remarkably affect the device performance, reliability, and lifetime, which are key features in practical applications, especially those in harsh environmental conditions [28]. With the aim of contributing to the assessment of the impact of the temperature on GaAs and GaN technologies, this article presents a comparative investigation of the temperature-dependent high-frequency behavior of two HEMTs based on AlGaAs/GaAs and AlGaN/GaN heterojunctions. To enable this comparative investigation, a sensitivity-based analysis is developed. The assessment of the sensitivity of the two HEMTs to changes in the ambient temperature (Ta) has been accomplished by using equivalent circuit models extracted from scattering (S-) parameters. The ambient temperature has been swept over a wide range of values, going from −40 ◦C to 150 ◦C. The bias point has been selected in order to allow, as much as possible, a fair comparison between the two different transistor technologies. The GaAs and GaN HEMTs have the same gate width of 200 µm but differ in the gate lengths, which are 0.25 µm and 0.5 µm, respectively. For the first time, the challenging task of comparing the temperature-dependent performance of the two different semiconductor technologies is accomplished by reporting an extensive and systematic sensitivity-based analysis, which is carried out by using the drain current (Ids), the equivalent-circuit parameters (ECPs), and the major RF figures of merit. The degradations of the device performance at a higher Ta are found to be more pronounced for the GaN technology, which can be attributed to the higher dissipated power (Pdiss). It is worth noting that the two tested technologies are inherently different and that this then clearly impacts on the achieved results. Given the widely different characteristics of the two tested technologies, it is really not feasible to distinguish each contribution arising from the different operating conditions (e.g., dissipated power) and peculiar device physics (e.g., thickness and thermal conductivity of the substrate). Hence, the reported comparative analysis has not aimed at distinguishing each contribution but at assessing the overall impact of the ambient temperature on the DC and microwave characteristics of the two tested technologies. Nevertheless, for the sake of completeness, it should be underlined that the channel temperature is higher than the ambient temperature because of the heat generated by the self-heating effects, which are strongly dependent not only on the dissipated power level but also on the thickness and thermal conductivity of the materials [13,29–36]. Furthermore, it is worth mentioning that the extraction of the equivalent-circuit elements may be inevitable affected by the uncertainty inherent in measurements and that, in addition, the model topology itself is an approximation of the device physics [37–43], which in turn may impact on the achieved temperature-dependent findings.

The remainder of this article is organized as follows: Section 2 is focused on the description of the tested device and experiments, Section 3 is devoted to the sensitivitybased analysis and the discussion of the findings, and the last section summarizes the main conclusions of this study.

II. DEVICES AND EXPERIMENTS

The two studied devices are an AlGaAs/GaAs HEMT grown by molecular beam epitaxy (MBE) on a semi-insulating undoped GaAs substrate and an AlGaN/GaN HEMT grown by metal-organic chemical vapor deposition (MOCVD) on a SiC substrate. Figure 1 shows the schematic cross-sectional views and photos of the two tested HEMTs. The interdigitated layout of both devices is based on the connection in parallel of two fingers, each being 100-µm long, yielding to a total gate width of 200 µm. The gate lengths of the GaAs and GaN devices are 0.25 µm and 0.5 µm, respectively. The source-to-gate distance (LSG) and the gate-to-drain distance (LGD) are 0.5 µm and 2.0 µm for the GaAs device, while their values are equal to 1 µm and 2.75 µm for the GaN device.

The microwave experiment consists of S-parameters measured from 45 MHz to 50 GHz at nine different ambient temperatures: −40 ◦C, −25 ◦C, 0 ◦C, 25 ◦C, 50 ◦C, 75 ◦C, 100 ◦C, 125 ◦C, and 150 ◦C. The S-parameters were measured with a vector network analyzer (VNA HP8510C) in conjunction with a DC source (HP4142B) for biasing, a temperature control unit (Temptronic TP03200, Temptronic Corporation, Mansfield, MA, USA) for setting the ambient temperature, and a PC with a specialized software (IC-CAP) for controlling the full measurement procedure through the GPIB interface. The off-wafer calibration was performed using line-reflect-reflect-match (LRRM) standards on the alumina calibration substrate from Cascade Microtech and a commercial calibration software (WinCal). The comparative analysis is performed using S-parameters at the following two bias points in the saturation region: Vds = 3 V and Vgs = −0.1 V for the GaAs HEMT and Vds = 9 V and Vgs = −4 V for the GaN HEMT. This choice has been made based on the analysis of the DC output characteristics of the two transistors at different Ta (see Figures 2 and 3), in order to enable, as much as possible, a fair comparison between the two different technologies. For the GaAs HEMT, two temperature-dependent effects contribute in opposite ways to the resultant behavior of Ids with an increasing temperature: the degradation of the carrier transport properties and the threshold voltage (Vth) shift towards more negative values. Therefore, Vgs is selected at −0.1 V, in order to minimize the contribution of the Vth shift that plays a more dominant role at lower Vgs. Vds is selected at 3 V, in order to avoid the pronounced positive slope of Ids at high Vds. For the GaN HEMT, the temperature-dependent behavior of Ids is mostly due to the degradation of the carrier transport properties and/or to a reduction in the carrier concentration in the two-dimensional electron gas (2DEG). Therefore, Vds and Vgs are, respectively, selected at 9 V and −4 V, in order to avoid the pronounced negative slope of Ids (Vds) at a high Pdiss

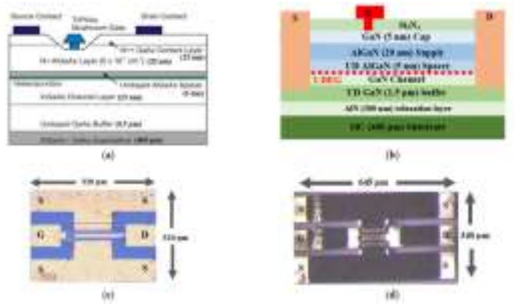

Figure 1. Schematic cross-sectional views and photos of the tested high electron-mobility transistors (HEMTs) based on (a,c) AlGaAs/GaAs and (b,d) AlGaN/GaN heterostructures.

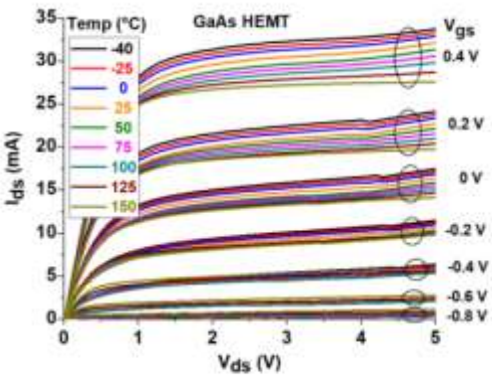

Fig:2 Dc output characteristics of the studied Ga as HEMT at different Ta

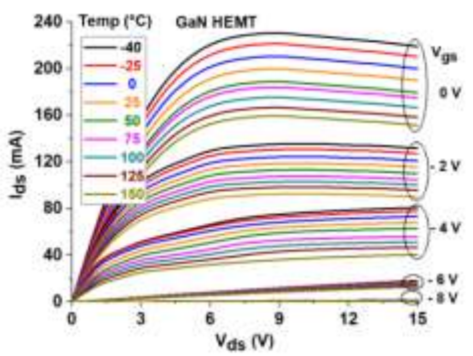

Figure 3. DC output characteristics of the studied GaN HEMT at different T_a

At the selected bias voltages (see Figure 4), the dimensionless relative sensitivity of Ids with respect to Ta is calculated by normalizing the relative change in Ids to the relative change in Ta:

$$RSI_{ds} = \frac{\Delta I_{ds}}{I_{ds0}}\frac{T_{a0}}{\Delta T_a} = \frac{(I_{ds} - I_{ds0})}{I_{ds0}}\frac{T_{a0}}{(T_a - T_{a0})} \quad (1)$$

Where Ids0 is the value of Ids at the reference temperature (Ta0) of 25 ◦C. As can be observed in Figure 4, RSId s is negative for both devices, as a consequence of the fact that an increase in Ta leads to a decrease in Ids, and is of greater magnitude for the GaN technology, as a consequence of the much higher Pdiss leading to a higher channel temperature (i.e., Tch = Ta + RthPdiss where Rth is the thermal resistance)

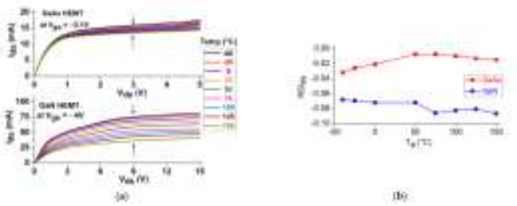

Figure 4. (a) The selected bias points for the sensitivity-based analysis are Vds = 3 V and Vgs = −0.1 V for the GaAs HEMT (top plot) and Vds = 9 V and Vgs = −4 V for the GaN HEMT (bottom plot); (b) Behavior of RSIds versus Ta for the studied (red line) GaAs and (blue line) GaN HEMTs.

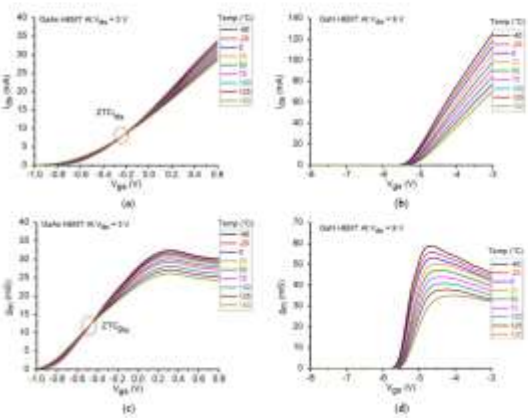

Figure 5. DC transcharacteristics and transconductances at different Ta for (a,c) the GaAs HEMT at Vds = 3 V nd (b,d) the GaN HEMT AT V_{DS} =9V

Figure 6 shows the impact of Ta on the measured S-parameters at the selected bias points. By increasing Ta, the low-frequency S21 is reduced, due to the degradation of the carrier transport properties. Both devices are affected by the kink effect in S22 [44–49], which is more marked at a lower Ta because of the higher gm. As a matter of fact, it has been demonstrated that the kink effect is mainly due to high values of gm.

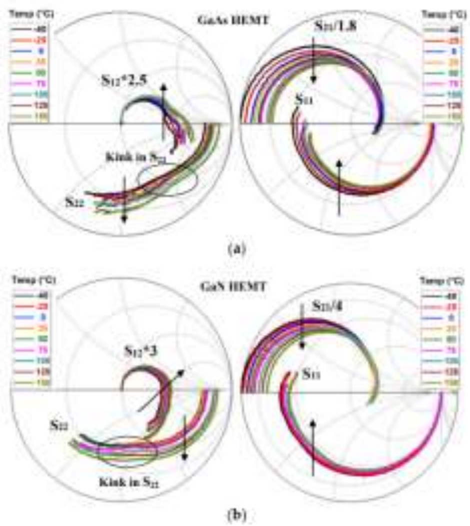

Figure 6. Measured S-parameters of the studied (a) GaAs and (b) GaN HEMTs at different Ta. The illustrated bias points are: Vds = 3 V and Vgs = −0.1 V for the GaAs HEMT and Vds = 9 V and Vgs = −4 V for the GaN HEMT. The frequency range goes from 45 MHz to 50 GHz. ("*" means product (the multiplication operation)).

III. SENSITIVITY-BASED ANALYSIS

The S-parameters have been modelled using the equivalent-circuit model in Figure 7. The ECPs have been obtained by using a standard "cold" pinch-off approach [50]. As illustrated in Figure 8, a good agreement between the measured and simulated S-parameter has been achieved for the two tested devices. Electronics 2021, 10, x FOR PEER REVIEW illustrated in Figure 8, a good agreement

ISSN: 2096-3246
Volume 54, Issue 06, Nov 2022

between the measured and simulated Seter has been achieved for the two tested devices

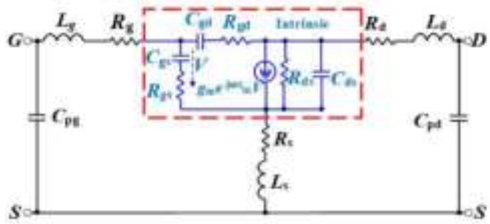

Figure 7. Equivalent-circuit model for the studied GaAs and GaN HEMTs

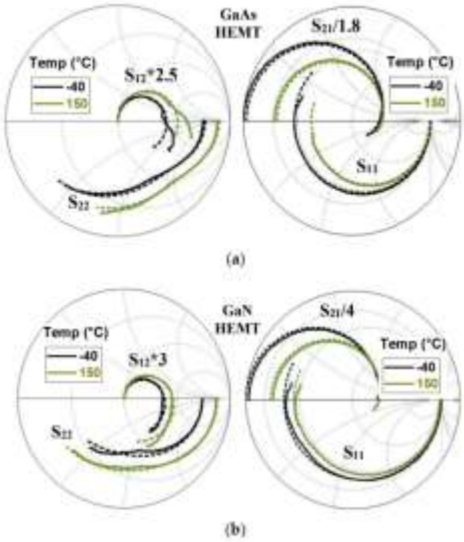

Measured S-parameters of the studied (a) GaAs and (b) GaN HEMTs at different Ta. The illustrated bias points are: Vds = 3 V and Vgs = −0.1 V for the GaAs HEMT and Vds = 9 V and Vgs = −4 V for the GaN HEMT. The frequency range goes from 45 MHz to 50 GHz. ("*" means product (the multiplication operation)).

Table 1 reports the values of the drain current, the ECPs, the intrinsic input and feedback time constants (i.e., τgs = RgsCgs and τgd = RgdCgd), the unity current gain cut-off frequency (ft), and the maximum frequency of oscillation (fmax). The three intrinsic time constants (τm, τgs, and τgd) model the intrinsic non-quasi-static (NQS) effects, which arise from the inertia of the intrinsic device in responding to rapid signal changes [51]. The values of ft and fmax are, respectively, determined from the measured short-circuit current gain (h21) and maximum stable/available gain (MSG/MAG). Although the GaAs HEMT has a shorter gate length that should result in a higher operation frequency, the GaN HEMT has smaller time constants (except for τgd) and higher ft and fmax, which are desired in order to enable device applications at high frequencies. This is can be linked to the fact that the conventional scaling rules cannot be directly applied to make a straightforward comparison between devices that are based on different semiconductor materials, technologies, and layouts. As a matter of fact, this could be foreseen from the values of Ids, which are larger for the GaN HEMT, even if the GaAs HEMT has a shorter gate length that should result in a higher Ids. The same observation can be made for the intrinsic gm.

Likewise, in the case of Ids, the relative sensitivities of the other parameters in Table 1 are estimated by using Equation (1) and are then illustrated in Figures 9–11. Relative sensitivities of the extrinsic capacitances and inductances of close to zero were achieved (see Figure 9a–e), owing to their weak temperature dependence. On the other hand, the relative sensitivities of the extrinsic and intrinsic resistances are positive (see Figures 9f–h and 10d–f), due to the increase of the resistive contributions with an increasing Ta. Contrary to the resistances, the transconductance shows a relative sensitivity that is negative (see Figure 11a), enlightening its degradation with an increasing Ta. The relative sensitivities of the intrinsic capacitances can be positive or negative (see Figure 10a–c), depending on the considered device and capacitance. The relative sensitivities of the intrinsic time constants are positive (see Figure 11b–d), reflecting their increase at a higher Ta and thus a shift of the onset of the NQS effects at lower frequencies. On the other hand, the relative sensitivities of the frequencies ft and fmax are negative (see Figure 11e,f), reflecting their decrease at a higher Ta and thus a reduction of the device operation frequencies. The analysis of the relative sensitivities of the crucial parameters such as gm, ft , and fmax shows that larger negative values are observed for the GaN device compared to the GaAs counterpart (see

Figure 11a,e,f), in line with what was seen for Ids (see Figure 4).

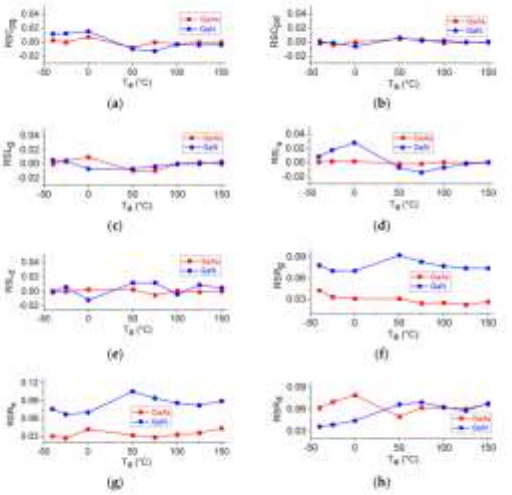

Figure 9. Behavior of the relative sensitivities of the extrinsic parameters versus Ta for the two studied devices. Figure 9. Behavior of the relative sensitivities of the extrinsic parameters versus Ta for the two studied devices.

Table 1. Parameters for GaAs and GaN HEMTs at 25 ◦C.

Parameters	GaAs HEMT	GaN HEMT
I_{ds} (mA)	14.7	63.5
C_{pg} (fF)	13.1	32.0
C_{pd} (fF)	41.6	30.0
L_g (pH)	104.0	142.0
L_s (pH)	5.41	1.43
L_d (pH)	37.8	84.0
R_g (Ω)	2.3	2.7
R_s (Ω)	4.0	3.1
R_d (Ω)	6.3	8.2
C_{gs} (fF)	275.0	199.9
C_{gd} (fF)	30.4	26.9
C_{ds} (fF)	55.9	89.2
R_{gs} (Ω)	1.5	1.2
R_{gd} (Ω)	6.3	13.0
R_{ds} (Ω)	360.0	322.4
g_m (mS)	29.6	63.0
τ_m (ps)	3.8	1.8
τ_{gs} (ps)	2.6	1.5
τ_{gd} (ps)	1.2	2.2
f_t (GHz)	14.9	40.0
f_{max} (GHz)	44.8	97.0

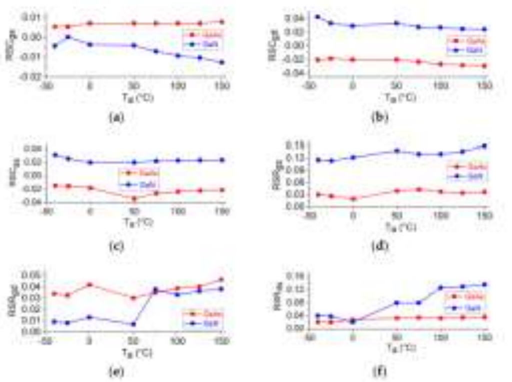

Figure 10. Behavior of the relative sensitivities of the intrinsic resistances and capacitances versus Ta for the two studied devices. The illustrated bias points are: Vds = 3 V and Vgs = −0.1 V for the GaAs HEMT and Vds = 9 V and Vgs = −4 V for the GaN HEMT.

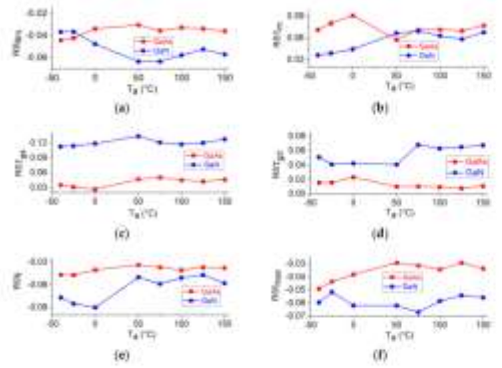

Figure 11. Behavior of the relative sensitivities of the intrinsic transconductance, the intrinsic time constants, and the RF figures of merit versus Ta for the two studied devices. The illustrated bias points are: Vds = 3 V and Vgs = −0.1 V for the GaAs HEMT and Vds = 9 V and Vgs = −4 V for the GaN HEMT.

IV. CONCLUSIONS

A comprehensive and methodical comparative analysis of GaAs and GaN HEMT technologies was conducted, examining the effects of temperature variations on device performance. The study focused on the relative sensitivities of Ids, ECPs, and major RF figures of merit across a wide temperature range, from -40 ◦C to 150 ◦C. When the temperature (Ta) is increased, both devices experience a decrease in performance. However, this decrease is more significant for the GaN technology. This phenomenon may be ascribed to the elevated Pdiss, which results in a more pronounced deterioration of the electron transport characteristics. It is important to note that comparing the temperature-dependent performance of semiconductor technologies that are inherently different is a difficult task. This is because it is challenging to define consistent operating conditions for devices that have varying performances. For example, the current density needs to be considered for each technology being tested, and it is also difficult to separate the effects of different features, such as the thermal conductivities of the substrates. Therefore, the choice of bias circumstances that are substantially balanced has been determined by analyzing the particular DC output characteristics. These settings are then utilized as a reference point to evaluate the overall effect of Ta on the microwave properties of the two devices. The selection of the relative sensitivity as an assessment indicator is based on its ability to provide a quantitative, systematic, and direct evaluation of the influence of Ta on the microwave properties. While the obtained results may not be universally applicable due to the influence of various factors in ECPs, which can vary depending on the specific device, the research methodology is independent of technology and can be directly used to compare other FETs in a quantitative and systematic manner.

REFERENCES

1. Mimura, T.; Hiyamizu, S.; Fujii, T.; Nanbu, K. A new field-effect transistor with selectively doped GaAs/n-AlxGa1-x as heterojunctions. Jpn. J. Appl. Phys. 1980, 19, L225–L227. [CrossRef]

2. Khan, M.A.; Bhattarai, A.; Kuznia, J.N.; Olson, D.T. High electron mobility transistor based on a GaN-AlxGa1-xN heterojunction. Appl. Phys. Lett. 1993, 63, 1214–1215. [CrossRef]

3. Belache, A.; Vanoverschelde, A.; Salmer, G.; Wolny, M. Experimental analysis of HEMT behavior under low-temperature conditions. IEEE Trans. Electron Dev. 1991, 38, 3–13. [CrossRef]

4. Anholt, R.E.; Swirhun, S.E. Experimental investigation of the temperature dependence of GaAs FET equivalent circuits. IEEE Trans. Electron Dev. 1992, 39, 2029–2036. [CrossRef]

5. Marinkovic, Z.; Markovic, V. Temperature-dependent models of low-noise microwave transistors based on neural networks. Int. J. RF Microw. Comput. Aided Eng. 2005, 15, 567–577. [CrossRef]

6. Caddemi, A.; Crupi, G.; Donato, N. On the soft breakdown phenomenon in AlGaAs/InGaAs HEMT: An experimental study down to cryogenic temperature. Solid State Electron. 2005, 49, 928–934. [CrossRef]

7. Caddemi, A.; Crupi, G.; Donato, N. Temperature effects on DC and small signal RF performance of AlGaAs/GaAs HEMTs. Microelectron. Reliab. 2006, 46, 169–173. [CrossRef]

8. Huang, J.C.; Hsu, W.C.; Lee, C.S.; Huang, D.H.; Huang, M.F. Temperature-dependent characteristics of enhancement-/depletionmode double-doped AlGaAs/InGaAs pHEMTs and their monolithic DCFL integrations. Solid State Electron. 2007, 51, 882–887. [CrossRef]

9. Zhu, Y.; Karalkar, S.; Prasad, K.; Wei, C.; Mason, J.; Bartle, D. Temperature dependent linear HEMT model extracted with multi-temperature optimization. In Proceedings of the Asia Pacific Microwave Conference, Kaohsiung, Taiwan, 4–7 December 2012; pp. 756–759. [CrossRef]

10. Alim, M.A.; Rezazadeh, A.A. Temperature-dependent DC and small-signal analysis of AlGaAs/InGaAs pHEMT for high frequency applications. IEEE Trans. Electron Dev. 2016, 63, 1005–1012. [CrossRef]

11. Alim, M.A.; Rezazadeh, A.A. Device behaviour and zero temperature coefficients analysis for microwave GaAs HEMT. Solid State Electron. 2018, 147, 13–18. [CrossRef]

12. Alim, M.A.; Rezazadeh, A.A.; Crupi, G. Experimental insight into the temperature effects on DC and microwave characteristics for a GaAs pHEMT in multilayer 3-D MMIC technology. Int. J. RF Microw. Comput. Aided Eng. 2020, 30, e22379. [CrossRef]

13. Gryglewski, D.; Wojtasiak, W.; Kami ´nska, E.; Piotrowska, A. Characterization of self-heating process in GaN-based HEMTs. Electronics 2020, 9, 1305. [CrossRef]

14. Camarchia, V.; Cappelluti, F.; Pirola, M.; Guerrieri, S.D.; Ghione, G. Self-consistent electrothermal modeling of class A, AB, and B power GaN HEMTs under modulated RF excitation. IEEE Trans. Microw. Theory Tech. 2007, 55, 1824–1831. [CrossRef]

ISSN: 2096-3246
Volume 54, Issue 06, Nov 2022

15. Darwish, A.M.; Huebschman, B.D.; Viveiros, E.; Hung, H.A. Dependence of GaN HEMT millimeter-wave performance on temperature. IEEE Trans. Microw. Theory Tech. 2009, 57, 3205–3211. [CrossRef]

16. Vitanov, S.; Palankovski, V.; Maroldt, S.; Quay, R. High-temperature modeling of AlGaN/GaN HEMTs. Solid State Electron. 2010, 54, 1105–1112. [CrossRef]

17. Crupi, G.; Avolio, G.; Raffo, A.; Barmuta, P.; Schreurs, D.M.M.-P.; Caddemi, A.; Vannini, G. Investigation on the thermal behavior for microwave GaN HEMTs. Solid State Electron. 2011, 64, 28–33. [CrossRef]

18. Angelotti, A.M.; Gibiino, G.P.; Florian, C.; Santarelli, A. Trapping dynamics in GaN HEMTs for millimeter-wave applications: Measurement-based characterization and technology comparison. Electronics 2021, 10, 137. [CrossRef]

19. Marinkovi´c, Z.; Crupi, G.; Caddemi, A.; Avolio, G.; Raffo, A.; Markovi´c, V.; Vannini, G.; Schreurs, D.M.M.-P. Neural approach for temperature dependent modeling of GaN HEMTs. Int. J. Numer. Model. Electron. Netw. Devices Fields 2015, 28, 359–370. [CrossRef]

20. Crupi, G.; Raffo, A.; Avolio, G.; Schreurs, D.M.M.-P.; Vannini, G.; Caddemi, A. Temperature influence on GaN HEMT equivalent circuit. IEEE Microw. Wirel. Comp. Lett. 2016, 26, 813–815. [CrossRef]